Cyclotron-Produced Zn-62: Its Possible Use in Prostate and Pancreas Scanning as a Zn-62 Amino Acid Chelate

Y. Yano and T. F. Budinger

Donner Laboratory and Lawrence Berkeley Laboratory, University of California, Berkeley, California

Zinc-62 is a positron emitter that localizes in pancreas, prostate, and liver. Cyclotron-produced Zn-62 was separated by column chromatography and evaluated in vivo as the chelate of five amino acids and also as $^{62}ZnCl_2$. Tissue-distribution studies were done in normal animals from 0.7–23 hr after intravenous administration. Pancreas-to-liver ratios (per gram) of about 1.0 were found at 1.5 hr in studies on rats, dogs, and monkeys. Pancreas was as difficult to separate from liver in Zn-62 (amino acid) images as in [^{75}Se] selenomethionine images. Some studies were done with Zn-65 to determine the effects of carrier zinc and molar ratios of ligand. The highest ratio of pancreas to liver in these studies was 1.44. This uptake ratio decreases with increasing amounts of histidine, but the ratio is increased by adding carrier zinc because there results a decrease in liver uptake and no change in the pancreas uptake. There is sufficient specificity of pancreas and prostate uptake to make feasible emission computed tomography with Zn-62.

J Nucl Med 18: 815–821, 1977

Cyclotron-produced Zn-62, a positron emitter, has potential application to positron reconstruction tomography in the imaging of the pancreas or prostate. The present study compares the uptakes in target organs (prostate, pancreas, and liver) of $^{62}ZnCl_2$ and various amino acid chelates at high specific activity.

Zinc is known to accumulate in the islet cells of the pancreas and in the prostate, possibly as a metalloenzyme. A number of studies have been done with Zn-65, Zn-69m, and Zn-62 in animals and humans to image the prostate and to determine the in vivo distribution of zinc radionuclides, usually as the chloride (*1–9*). Previous studies of the distribution of zinc in man include 18 necropsy studies wherein $^{65}ZnCl_2$ ($T_{1/2}$ = 245 days) was injected before death, and 36 others in which biopsy samples were analyzed (*1,2*). The liver had the highest uptake, 0.05% injected dose/g. Pancreas was the next highest with an uptake of about 0.01% dose/g; the prostate absorbed about 0.005% dose/g and skeletal muscle about 0.002% dose/g. These tissue studies were corroborated by imaging investigations using $^{69m}ZnCl_2$ (14 hr, 439 keV), wherein the high liver uptake was observed and whole-body loss was found to be low, with less than 5% excretion by feces and urine at 5 days (*3,4*). The normal or hypertrophied prostate has been shown to have sufficient zinc uptake for imaging (*5*), but the prostatic uptake is variable, with fluctuations as much as sevenfold as determined by autoradiography.

Most of the studies with zinc isotopes have emphasized the prostate, with little attention to the potential of zinc in imaging the pancreas. Early studies (*10*) showed a pancreas-to-liver ratio of about 1.0 in the rat using $^{65}ZnCl_2$, but improved ratios of 1.0–3.6 were found using Zn-65 chelated

Received July 21, 1976; revision accepted March 11, 1977.

For reprints contact: Yukio Yano, Donner Lab., University of California, Berkeley, Berkeley CA 94720.

to glycine (*6*). Studies in man (*1,2*) gave a pancreas-to-liver ratio of 0.2 with $^{65}ZnCl_2$. Zinc is found mainly in the islets of Langerhans in the cytoplasm of α and β cells, where zinc has an important role in the elaboration of insulin and glucagon (*7*). The fact that carrier $^{65}ZnCl_2$ uptake per gram of liver is equal to or greater than that in the pancreas would argue against attempts to image the pancreas. We speculated, however, that the pancreas-to-liver and prostate-to-muscle or blood ratios for zinc uptake might be markedly improved by administration of high-specific-activity zinc and/or chelation of zinc with an amino acid. Our experiments in rats, dogs, and monkeys show that this is not the case, yet Zn-62 does have a potential role with positron-emission tomographic devices for quantitating islet-cell distribution or activity and for some metabolic activities of the prostate.

MATERIALS AND METHODS

Zinc-62 ($T_{1/2}$ = 9.3 hr) decays 80% by EC and 20% by $\beta+$ emission (660 keV_{max}); the 9.8-min Cu-62 daughter decays 97% by $\beta+$ emission (2.91 MeV_{max}) and 2% by EC, yielding stable Ni-62. In addition to the 511-keV annihilation radiation, Zn-62 emits gamma photons at 590 keV (22%) and 42 keV (20%), while the Cu-62 daughter gives photons of 880 keV (0.3%), and 1.19 MeV (5%) in addition to the annihilation photons.

Zinc-62 was produced by irradiating 0.13-mm-thick copper foil with 30-MeV protons at the Lawrence Berkeley Laboratory (LBL) 88-in. cyclotron. The average beam current was 10–15 μA with an integrated beam of 25 μAh. The production yield was about 1 mCi/μAh at the end of irradiation. The copper target was allowed to "cool" for 4–5 hr to permit the short-lived copper and zinc contaminants to decay before chemical processing was begun.

The copper target foil was brought into solution with a minimum volume of 1:1 HNO_3 with gentle heating. The HNO_3 acid solution was evaporated to near dryness on a hot plate and under a heated nitrogen stream. Concentrated hydrochloric acid was added and the solution was again taken to near dryness. The residue of $CuCl_2$–$^{62}ZnCl_2$ was brought into solution with 2.5 *M* HCl and passed through a 1-cm-diam × 10-cm-high column of AG 1 × 8, 100–200-mesh, anion-exchange resin that had been prewashed with 2.5 *M* HCl. The resin column was then washed with an additional 50 ml of 2.5 *M* HCl. The Zn-62 remaining on the resin column was eluted with 50 ml of sterile water, which was collected in 10-ml fractions. Most of the "no carrier" added $^{62}ZnCl_2$ activity was found in fractions 2–4. Ten to twenty milligrams of the amino acid of interest were added to the $^{62}ZnCl_2$ in a 10-ml H_2O solution. The pH was adjusted to 5.5–6.0 with dilute NaOH or $NaHCO_3$ and the solution was passed through an 0.22-μm mem-

TABLE 1. UPTAKE OF Zn-62 AMINO ACID AND CHLORIDE IN NORMAL RATS*

	Δt (hr)	Blood	Liver	Kidneys	Spleen	Pancreas	Prostate	Muscle	Pancreas Liver	Prostate Muscle
Alanine	1.5	0.22	2.74	2.84	1.35	1.51	0.40	0.12		
		(0.17–0.30)	(1.70–4.39)	(2.02–3.94)	(1.11–1.75)	(1.24–1.90)	(0.28–0.46)	(0.08–0.19)	0.55	3.33
	20	0.14	1.26	0.91	1.10	0.90	0.93	0.22		
		(0.12–0.16)	(1.05–1.45)	(0.79–1.10)	(0.91–1.24)	(0.50–1.15)	(0.36–1.24)	(0.13–0.28)	0.71	4.23
Cysteine	1.5	0.21	2.20	2.41	1.27	1.59	0.66	0.08		
		(0.18–0.23)	(2.08–2.35)	(1.92–2.94)	(1.14–1.50)	(1.49–1.69)	(0.43–0.77)	(0.07–0.09)	0.72	8.25
	20	0.10	0.91	0.74	0.74	0.43	1.05	0.11		
		(0.08–0.11)	(0.79–1.07)	(0.68–0.86)	(0.66–0.82)	(0.27–0.51)	(0.81–1.47)	(0.09–0.12)	0.47	9.55
Histidine	1.5	0.30	2.71	3.08	1.45	2.32	0.71	0.19		
		(0.29–0.32)	(2.32–2.96)	(2.74–3.46)	(1.07–1.91)	(2.18–2.51)	(0.54–0.93)	(0.18–0.20)	0.86	3.74
	20	0.19	1.40	1.30	1.29	1.07	1.19	0.21		
		(0.16–0.21)	(1.30–1.48)	(1.01–1.56)	(1.15–1.40)	(0.98–1.26)	(1.02–1.39)	(0.19–0.23)	0.76	5.70
Tryptophan	1.5	0.21	2.11	2.29	1.22	1.58	0.40	0.07		
		(0.19–0.22)	(2.03–2.15)	(2.07–2.41)	(1.07–1.32)	(1.00–2.14)	(0.10–0.63)	(0.02–0.12)	0.75	5.71
	20	0.15	1.19	1.23	1.10	0.91	1.06	0.18		
		(0.12–0.21)	(1.00–1.48)	(0.79–2.02)	(0.79–1.59)	(0.62–1.15)	(1.01–1.11)	(0.13–0.25)	0.76	5.89
Arginine	1.5	0.19	2.29	2.43	1.52	2.44	0.64	0.14		
		(0.14–0.25)	(2.07–2.62)	(1.86–3.04)	(1.19–1.81)	(1.78–3.15)	(0.38–0.98)	(0.12–0.16)	1.07	4.57
	20	0.12	1.03	0.83	0.93	0.66	0.93	0.16		
		(0.12–0.13)	(0.92–1.16)	(0.74–0.90)	(0.89–0.96)	(0.59–0.77)	(0.52–1.38)	(0.15–0.17)	0.64	5.81
Chloride	1.5	0.46	2.66	3.44	1.78	2.46	0.57	0.19		
		(0.35–0.69)	(2.42–2.90)	(3.28–3.52)	(1.58–1.96)	(2.16–2.76)	(0.46–0.68)	(0.19–0.19)	0.92	3.00
	20	0.15	1.48	1.10	1.13	0.96	0.94	0.20		
		(0.12–0.17)	(1.05–1.90)	(0.81–1.30)	(0.85–1.44)	(0.55–1.29)	(0.78–1.16)	(0.12–0.26)	0.78	4.70

* %/g Mean of 3–4 (range).

brane filter. More than 95% of the Zn-62 activity was in the filtrate. The amounts of copper and zinc in the preparations were determined by spectrochemical analysis.

Five amino acids were used (as the hydrochloride or the free base) to form the Zn amino acid chelates; these ligands were alanine, arginine, cysteine, histidine, and tryptophan.* The chelates were administered to tumor-bearing mice and to normal rats, dogs, and monkeys. In addition, $^{62}ZnCl_2$ at pH 2–3 was used in similar studies to compare liver uptake relative to pancreas uptake.

Studies were done with normal male Sprague-Dawley rats (250–350 g) to determine relative uptake at various times (0.7, 1.5, and 19–23 hr) after intravenous administration.

The kinetics of Zn-62 histidine distribution were also determined in male beagle dogs (~12 kg) at 3 and 17 hr after intravenous injection of 200 μCi. One-milliliter blood samples were taken at frequent intervals and counted in a NaI(*Tl*) well counter. After imaging the prostate of the dog with the Anger positron camera, the relative concentrations in the various organs were determined by killing the dog and counting the organs.

Zinc-62 amino acid uptake in the pancreas of a monkey, at 60 min after injection, was determined first by imaging the pancreas and liver with a scintillation camera equipped with a heavy lead pinhole collimator carrying a ⅜-in. platinum insert. The liver was then imaged with Tc-99m sulfur colloid. By computer processing, the liver shadow was subtracted from the first image, thus providing a Zn-62 histidine image of the pancreas alone. For comparison, another difference image of the pancreas was obtained in the same animal using [^{75}Se] selenomethionine and Tc-99m sulfur colloid.

In a second study, Zn-62 arginine was used to image the pancreas of a monkey 1 hr after intravenous administration of 700 μCi of activity. The pancreas–liver image was obtained, and the pancreas could be seen here without subtraction of the liver shadow. Immediately after the imaging procedure, a laparotomy was performed and the relative positions of the organs were used to check the scintiscans. Biopsy samples of pancreas, liver, and duodenum were obtained for counting.

To determine the effect of carrier zinc and molar ratios of ligand to zinc, $^{65}ZnCl_2$ was administered intravenously at pH 2–3 to 300-g rats using 30 and 213 μg of stable zinc per kg rat. The uptake in the various organs was determined at 1.5 and 23 hr after injection. Similarly Zn-62 histidine uptake at 2:1 and 10:1 molar ratios of ligand to zinc was determined.

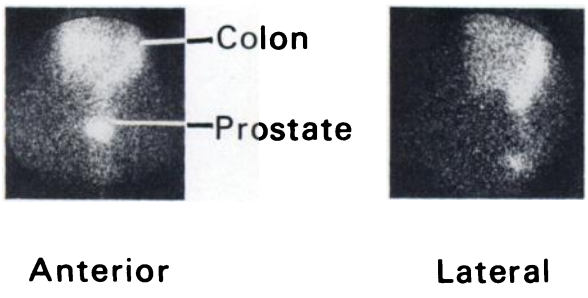

FIG. 1. Uptake of Zn-62 histidine in beagle dog 17 hr after iv administration of 200 μCi. Anger positron-camera image shows uptake in prostate and colon, in anterior and lateral views. Identification of prostate was made at necropsy.

RESULTS

Our initial studies with Zn-62 histidine were done because of the relatively high stability constant of the chelate (log K-12.9), and because of the high molar ratio of histidine to other amino acids in the prostate (*11*). For pancreatic imaging, however, the high liver uptake of histidine—as shown in our study and by autoradiography with a C-14 label (*12*)—is a disadvantage, and this caused us to look at the Zn-62 chelates of other amino acids, such as arginine. Stability constants (log K) for the amino acids we examined (*13,14*) are as follows: alanine 9.5, arginine 7.3, cysteine 18.6, histidine 12.9, and tryptophan 9.3.

Table 1 shows the uptakes in pancreas and prostate for the Zn-62 chelates of various amino acids—in normal rats at 1.5 and 20 hr after injection. The pancreas-to-liver concentration ratios were 0.86 for histidine, 1.1 for arginine, and 0.92 for $^{62}ZnCl_2$. The prostate uptake was greatest for histidine (1.19% dose/g), compared with 1.06%/g for tryptophan and 0.94%/g for zinc chloride, with prostate-to-muscle concentration ratios of 5.7, 5.9, and 4.7 respectively. Nevertheless, Zn-62 cysteine gave the highest prostate-to-muscle ratio (9.6), even though the uptake (1.05%/g) was lower than that for histidine.

The maximum uptake in pancreas was reached at 1.5 hr after injection, whereas the maximum uptake in liver was at 0.7 hr. For the prostate the highest uptake occurred at 20 hr.

Figure 1 shows anterior and lateral scintiscans (with the Anger positron camera) of uptake in the prostate and colon of a beagle dog, 17 hr after intravenous administration of 200 μCi of Zn-62 histidine. Immediately after the imaging the dog was sacrificed and the individual organs were removed and counted under the positron camera. About 30 min elapsed between organ removal and counting; thus the distribution is for Zn-62 as any Cu-62 which

might have been redistributed before animal sacrifice would have decayed. These data, shown in Table 2, confirm the prostate image because the uptake in the field of view was essentially only in the prostate and colon, and their relative positions with respect to each other at necropsy agreed with the positron picture. A second study gave similar results. The prostate-to-gut concentration ratios were 1.0 and 1.9 for the 2- and 17-hr periods, respectively. In dogs the pancreas-to-liver ratio increases nearly twofold with time from 2 hr to 17 hr after intravenous administration, which suggests a slower uptake of Zn-62 histidine in dogs than in rats. This change in uptake may be related more to dietary history and insulin production in the subject than to a species difference.

The dog's clearance curve for whole blood has two components, with half-times of 3.5 and 39 min. About 5% of the injected dose was in whole blood 70 min after intravenous injection.

Two subhuman primate studies (Figs. 2 and 3) show uptake in the pancreas in studies at 1 hr after intravenous injection of 700 μCi of Zn-62 histidine and Zn-62 arginine. Prostate studies were done 24 hr after injection and yielded results similar to those from the beagles. The pancreas image was enhanced by subtraction processing in which Tc-99m sulfur colloid was used to remove the liver image. This

TABLE 2. Zn-62 HISTIDINE DISTRIBUTION

	12.3-kg male beagle after 2 hr		11.8-kg male beagle after 24 hr	
	% activity per organ	% activity per g (× 100)	% activity per organ	% activity per g (× 100)
Pancreas	1.7	4.6	2.7	9.3
Liver	43.1	7.5	32.3	8.7
Prostate	0.2	2.7	0.4	6.2
Kidneys	3.5	3.3	2.2	2.6
Gut	14.7	2.8	16.0	3.5
Colon	0.8	0.4	4.0	4.6
Stomach	17.5	1.2	2.0	1.7
Heart	1.4	0.7	1.6	1.2
Lungs	1.0	0.6	1.2	1.1
Spleen	1.0	2.0	0.9	0.6
Carcass	27.0	0.3	37.0	0.4
Testes	0.07	0.4	—	—
Pancreas/Liver		0.6		1.1
Prostate/Gut		1.0		1.8

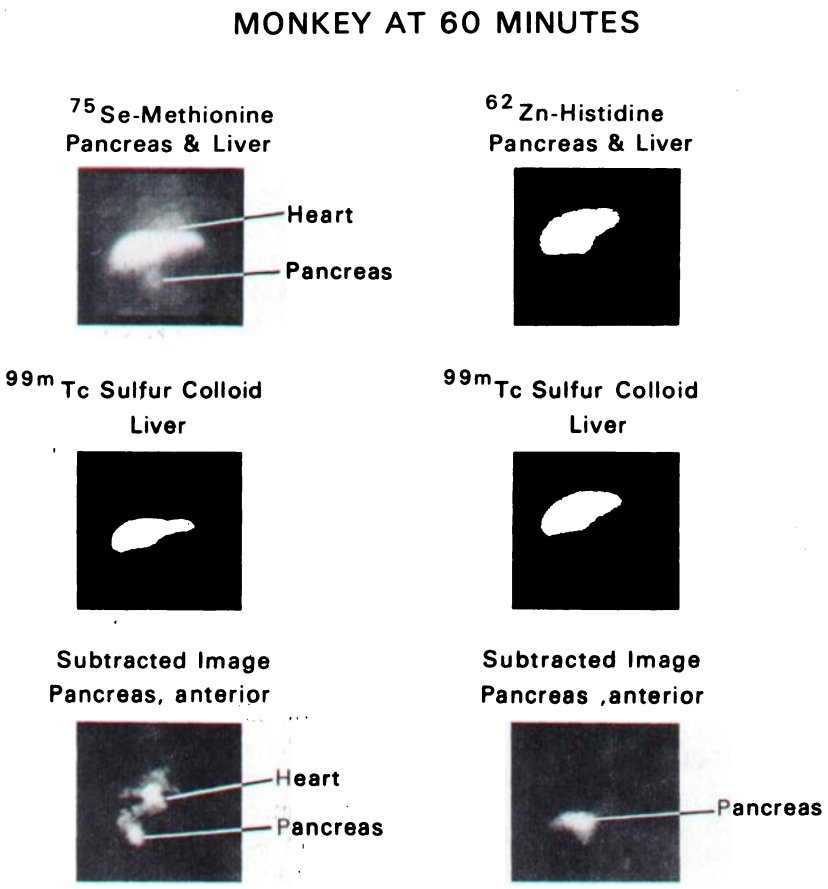

FIG. 2. Scintillation camera images (with pinhole collimator) of pancreas of monkey 1 hr after 700 μCi of Zn-62 histidine with Tc-99m sulfur colloid liver uptake subtracted by computer processing. Same technique was used with [^{75}Se] selenomethionine as comparison. Uptake in heart is seen in the Se-75 image; abnormal appearance of Zn-62 in pancreas thought to result from islet-cell distribution.

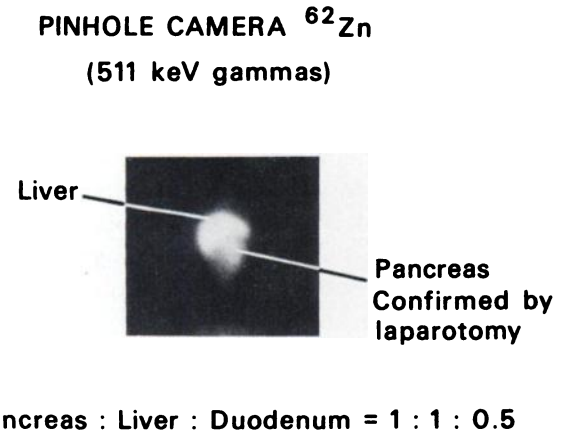

FIG. 3. Pancreatic image in a monkey (scintillation camera with pin hole collimator) 1 hr after iv injection of 700 μCi of Zn-62 arginine.

study was compared with a standard [^{75}Se] selenomethionine and Tc-99m sulfur colloid study in the same animal. The uptake of [^{75}Se] selenomethionine in the heart has been observed by us in other studies.

Zinc-62 arginine was administered to a second monkey and the liver-and-pancreas image was obtained as before but without liver subtraction. Figure 3 shows uptake in the pancreas; this was confirmed by counting biopsy samples from pancreas, liver, and duodenum to give 1:1:0.5 ratios, respectively, for counts per gram of tissue.

DISCUSSION

The results of our experiments with high-specific-activity Zn-62 are not in complete agreement with those reported by other researchers (*9,10*) who used low-specific-activity $^{65}ZnCl_2$. The relative uptakes in liver, pancreas, kidney, and prostate obtained in our study fall between those reported in the earlier work (*8–10*). The effect of carrier zinc in the $^{65}ZnCl_2$ preparations of those studies could markedly influence the in vivo uptake compared with the low-carrier Zn-62 in our studies. The amount of zinc in our Zn-62 preparations ranged from 1–2 μg Zn/kg rat. The zinc probably was an impurity in the copper-foil target, and there were variable amounts of carrier zinc, depending upon the H_2O fraction used from the recovery of Zn-62 from the anion-exchange resin. The later fractions from our resin column contained significantly smaller amounts of zinc, and were used in our Zn-62 preparations. This amount of carrier is insignificant compared with the amounts of zinc in low-specific-activity Zn-65 studies. Our results for Zn-65 distribution with 30 and 213 μg Zn/kg rat are shown in Table 3. An increase in the amount of carrier zinc by a factor of seven results in a decrease in the liver uptake of zinc, with no change in the pancreatic uptake. This results in a 60% improvement in pancreas-to-liver ratio at 1.5 hr (Table 3), while the uptake in prostate with the two zinc concentrations was unchanged at 1.5 and 23 hr. Thus, this experiment gives results contradicting the hypothesis that high-carrier preparations of radiozinc give relatively low pancreas-to-liver uptake ratios.

On the other hand, loading with the amino acid histidine appears to increase prostate uptake by as much as 20% (Table 4). The increase in molar ratio of histidine:zinc by a factor of five results in a 20% increase in the prostate:muscle concentration ratio of Zn-65 at 23 hr, with a 22% decrease in pancreatic activity at 1.5 hr.

For the imaging of the rat pancreas, Zn-62 arginine is superior to Zn-62 histidine or $^{62}ZnCl_2$ because the relative uptake of Zn-arginine is lower in the liver (Table 1). It might be possible to improve pancreas-to-liver concentration ratios by saturating the liver's binding sites with ionic carrier such as $ZnCl_2$ and then administering the Zn-62 arginine. The pancreas-to-liver concentration ratio can be in-

TABLE 3. $^{65}ZnCl_2$ UPTAKE IN NORMAL RATS*

Organ	%/gm at 1.5 hr		%/gm at 23 hr	
	Prep. A†	Prep. B‡	Prep. A†	Prep. B‡
Blood	0.17 (0.15–0.19)	0.23 (0.22–0.24)	0.09 (0.09–0.10)	0.10 (0.09–0.11)
Heart	0.45 (0.42–0.49)	0.42 (0.40–0.44)	0.41 (0.27–0.50)	0.44 (0.43–0.47)
Lungs	0.59 (0.58–0.60)	0.53 (0.52–0.55)	0.54 (0.50–0.60)	0.52 (0.45–0.56)
Liver	2.50 (2.02–3.10)	1.56 (1.53–1.59)	0.80 (0.78–0.83)	0.87 (0.85–0.91)
Kidneys	2.07 (1.68–2.60)	1.85 (1.66–2.19)	0.71 (0.63–0.78)	0.63 (0.61–0.64)
Spleen	1.13 (1.01–1.30)	0.83 (0.80–0.88)	0.66 (0.65–0.67)	0.66 (0.65–0.67)
Pancreas	2.25 (2.15–2.35)	2.24 (1.99–2.45)	0.54 (0.44–0.67)	0.54 (0.48–0.61)
Prostate	0.53 (0.42–0.71)	0.71 (0.63–0.83)	0.82 (0.69–0.98)	0.80 (0.59–0.90)
Sem. vesic.	0.16 (0.12–0.2)	0.26 (0.17–0.38)	0.25 (0.21–0.27)	0.30 (0.18–0.37)
%/g Pancreas / %/g Liver	0.90	1.44	0.68	0.62
%/g Prostate / %/g Blood	3.12	3.09	9.11	8.00

* Mean of three animals.
† Prep. A, 30 μg Zn/kg rat (avg. wt. 300 g).
‡ Prep. B, 213 μg Zn/kg rat (avg. wt. 300 g).

TABLE 4. Zn-65 HISTIDINE UPTAKE IN NORMAL RATS*

Organ	%/gm at 1.5 hr		%/gm at 23 hr	
	Prep. A†	Prep. B‡	Prep. A†	Prep. B‡
Blood	0.23 (0.22–0.24)	0.23 (0.22–0.23)	0.14 (0.12–0.16)	0.14 (0.12–0.15)
Heart	0.58 (0.51–0.62)	0.62 (0.47–0.70)	0.67 (0.59–0.78)	0.66 (0.62–0.70)
Lungs	0.89 (0.81–0.95)	0.85 (0.78–0.90)	0.77 (0.71–0.84)	0.75 (0.67–0.81)
Liver	2.82 (2.69–2.94)	2.87 (2.58–3.38)	1.48 (1.42–1.51)	1.30 (1.11–1.48)
Kidneys	2.83 (2.74–2.89)	2.93 (2.67–3.12)	0.98 (0.89–1.07)	1.01 (0.95–1.05)
Spleen	1.37 (1.22–1.50)	1.40 (1.21–1.56)	0.99 (0.93–1.09)	1.07 (1.02–1.10)
Pancreas	3.20 (3.18–3.23)	2.48 (2.16–2.67)	0.75 (0.57–0.95)	0.90 (0.82–1.02)
Prostate	0.66 (0.58–0.71)	0.76 (0.67–0.87)	1.29 (0.76–1.59)	1.54 (1.21–1.87)
Sem. vesic.	0.45 (0.41–0.50)	0.35 (0.26–0.42)	0.53 (0.42–0.74)	0.46 (0.36–0.55)
%/g Pancreas / %/g Liver	1.13	0.86	0.51	0.69
%/g Prostate / %/g Blood	2.87	3.30	9.21	11.0

* Mean of three animals (range).
† Prep. A, 2:1 histidine: Zn.
‡ Prep. B, 10:1 histidine: Zn.

creased by increasing the amounts of carrier zinc and by maintaining a minimal ratio of ligand to zinc, or by using a weakly bound ligand such as arginine. However, prostatic uptake of zinc can be increased by using either high molar ratios or ligands that bind zinc strongly, such as histidine or cysteine.

The difference in the appearance of pancreatic images obtained with [^{75}Se] selenomethionine and Zn-62 (amino acid), as in Fig. 2, might be explained by the fact that most of the zinc pool is in the islet cells, which are concentrated in the body and tail of the pancreas.

The radiation dose for Zn-62 has been calculated to be 0.8 rads/mCi whole body, 12 rads/mCi to each of liver, pancreas, and prostate, and 6 rads/mCi to kidneys in agreement with Chisholm et al. (*9*).

Satisfactory positron camera images of the prostate can be obtained about one day after injecting the 9-hr Zn-62 in rats, dogs, and monkeys. An enhanced prostate uptake of 20% was noted in rats by loading with histidine.

The pancreatic distribution of zinc is different from that of [^{75}Se] selenomethionine and this finding might be used to quantitate the metabolic state of the pancreas using positron tomographic devices. Further studies are needed to determine the best pancreas-to-liver ratio that can be obtained by combining carrier addition with an optimal ligand-to-zinc molar ratio. In transverse section imaging, the pancreas is separated from the liver; thus Zn-62 has potential for emission computed tomography with positron imaging systems.

ACKNOWLEDGMENTS

This work was supported by the U.S. Energy Research and Development Administration and by Research Grant 5RO1CA17566-02 RAD. The authors also thank Eugene P. Roth and Brian R. Moyer for technical assistance.

FOOTNOTE

* Calbiochem Corp., San Diego, Calif.

REFERENCES

1. SIEGEL E, GRAIG FA, CRYSTAL MM, et al.: Distribution of ^{65}Zn in the prostate and the organs of man. *Br J Cancer* 15: 647–664, 1961

2. SPENCER H, ROSOFF B, LEWIN I, SAMACHSON J: Studies of zinc-65 metabolism in man. In *Zinc Metabolism*, Prasad A, ed, Springfield, Ill, CC Thomas, 1966, pp 339–362

3. JOHNSTON GS, WADE MD, MURPHY GP, et al.: ^{65}Zn and ^{69m}Zn studies in the dog, monkey and man. *J Surg Res* 8: 528–534, 1970

4. BODDY K, EAST BW, KING PC, et al.: Preliminary studies of zinc metabolism in carcinoma of the prostate gland. *Br J Urol* 42: 475–480, 1970

5. GOLD FM, LORBER SA: Radioisotope ^{69m}Zn chloride prostate gland scan. I. ^{69m}Zn organ distribution studies and γ-camera scan in canine subjects. *Invest Urol* 8: 231–238, 1970

6. GREENLAW RH, STRAIN WH, CALLEAR TE, et al.: Experimental studies for scintillation scanning of the pancreas. *J Nucl Med* 3: 47–50, 1962

7. MIKAC-DEVIC D: Methodology of zinc determinations and the role of zinc in biochemical processes. *Adv Clin Chem* 13: 271–333, 1970

8. WAKELEY JCN, MOFFATT B, CROOK A, et al.: The distribution and radiation dosimetry of Zinc-65 in the rat. *Int J Appl Rad Isot* 7: 225–232, 1960

9. CHISHOLM GD, SHORT MD, CHANADIAN R, et al.: Radiozinc uptake and scinti-scanning in prostatic disease. *J Nucl Med* 15: 739–742, 1974

10. SHELINE GE, CHAIKOFF IL, JONES HB, et al.: Studies on the metabolism of zinc with the aid of its radioactive isotope. II. The distribution of administered radioactive zinc in the tissues of mice and dogs. *J Bio Chem* 139–151, 1943

11. HEATHCOTE JG, WASHINGTON RJ: Analysis of the zinc-binding protein derived from the human benign hyperthropic prostate. *J Endocrine* 58: 421–423, 1973

12. MATSUOKA DT, ALCARAZ AF, COHEN MB, et al.: Acute distribution of ^{14}C-amino acids in mice as determined by whole-body autoradiography: Adjunct for radiopharmaceutical synthesis. *Int J Appl Radiat Isot* 24: 705–707, 1973

13. SILLEN LG, MARTELL AB: *Stability Constants of Metal-Ion Complexes.* London, Burlington House, 1964

14. MARTELL AE, CALVIN M: *Chemistry of the Metal Chelate Compounds.* New York, Prentice-Hall, 1952

Accepted Articles to Appear in Upcoming Issues

Tc-99m Methylene Diphosphonate Versus Tc-99m Pyrophosphate: Biological and Clinical Comparison. Accepted 4/9/77.
Thomas G. Rudd, David R. Allen, and David E. Hartnett

Scintigraphic Diagnosis of Experimental Pulmonary Embolism with In-111-Labeled Platelets. Accepted 4/13/77.
Gaellan McIlmoyle, Harmon H. Davis, Michael J. Welch, Joan L. Primeau, Laurence A. Sherman, and Barry A. Siegel

Error Due to Radionuclide Decay During Rectilinear Scanning (Letter to the Editor). Accepted 4/18/77.
Richard P. Spencer and Fazle Hosain

Intraosseous Meningioma: An Unusual Radionuclide Presentation (Letter to the Editor). Accepted 4/20/77.
David Zaritzky and Robert J. Cowan

The Incorporation of Ga-67 into the Ferritin Fraction of Rabbit Hepatocytes In Vivo (Preliminary Note). Accepted 4/20/77.
Frederick N. Hegge, Delmar J. Mahler, and Steven M. Larson

Detection of Bronchopleural-Subarachnoid Fistula by Radionuclide Myelography (Case Report). Accepted 4/22/77.
Kenneth R. Hofstetter, John C. Bjelland, Dennis D. Patton, James M. Woolfenden, and Robert E. Henry

Sensitivity of Radionuclide Brain Scan in Cerebral Melioidosis (Case Report). Accepted 4/27/77.
David R. Brill and Jon D. Shoop

Visualization of Atrial Myocardium with Thallium-201 (Case Report). Accepted 4/27/77.
Michael J. Cowley, H. Cecil Coghlan, and Joseph R. Logic

The Measurement of 3-0 Methyldopamine in Urine and Plasma by a Rapid and Specific Radioimmunoassay. Accepted 4/27/77.
Bahjat A. Faraj, Vernon M. Camp, Albert W. Pruitt, James W. Isaacs, and Farouk M. Ali

Skeletal and Reticuloendothelial Imaging in Osteopetrosis (Case Report). Accepted 4/27/77.
Hee-Myung Park and John Lambertus

Tissue Distribution Studies with Radioactive Manganese: Potential for Myocardial Imaging (Preliminary Note). Accepted 4/27/77.
Depew M. Chauncey, Jr., Heinrich R. Schelbert, Samuel E. Halpern, Frank Delano, Martha L. McKegney, William L. Ashburn, and Phillip L. Hagan

A Comparison of Technetium-Etidronate and Pyrophosphate for Acute Myocardial Infarct Imaging. Accepted 4/27/77.
Craig C. Williams, Hiroshi Nishiyama, Robert J. Adolph, Donald W. Romhilt, Vincent J. Sodd, Eugene L. Saenger, and Marjorie Gabel

Comments on Tc-99m DTPA Scintillation Camera Renography (Letter to the Editor). Accepted 4/28/77.
Amnon Piepsz, Humphrey R. Ham, Andre Dobbeleir and Francois Erbsmann

Reply. Accepted 4/28/77.
S. P. Nielsen

New Tl-201 Nuclear Decay Data (Letter to the Editor). Accepted 4/28/77.
Harold W. Nass

Anatomic Patterns of Ga-67 Distribution in Localized and Diffuse Peritoneal Inflammation (Case Report). Accepted 4/28/77.
Paul J. Myerson, Daniel Myerson, and Richard P. Spencer

The Value of Bowel Preparation in Ga-67 Citrate Scanning (Concise Communication). Accepted 4/28/77.
Robert K. Zeman and Thomas W. Ryerson

Technetium-99 Glucoheptonate in Brain-Tumor Detection: An Important Advance in Radiotracer Techniques. Accepted 5/2/77.
Jean Leveille, Cesar Pison, Yousri Karakand, Raymond Lemieux, and Bertrand J. Vallieres

Technetium-99m-Labeled N-(2, 6-Dimethylphenylcarbamoylmethyl) Iminodiacetic Acid (Tc-99m HIDA): A New Radiopharmaceutical for Hepatobiliary Imaging Studies. Accepted 5/4/77.
James Ryan, Malcolm Cooper, Michael Loberg, Elizabeth Harvey, and Stephen Sikorski

Film-Loop Method for Cardiac Motion Images (Letter to the Editor). Accepted 5/4/77.
Philip D. Van Heerden, Willem P. Baard, Kobus Reynecke, and Helmuth Weich

Indium-111-Labeled Autologous Leukocytes in Man. Accepted 5/4/77.
Mathew L. Thakur, J. Peter Lavender, Rosemary N. Arnot, David J. Silvester, and Anthony W. Segal

Augmented Splenic Uptake of Tc-99m Sulphur Colloid in Malignant Melanoma (Letter to the Editor). Accepted 5/6/77.
Larry Nathanson and Paul Kahn

Ultrasound as a Complementary Procedure to Radionuclide Thyroid Scanning (Letter to the Editor). Accepted 5/6/77.
Ernest F. Crocker, Andrew F. McLaughlin, George J. Bautovich, and Roger F. Uren

Reply. (Accepted 5/6/77).
Roger C. Sanders

Method to Calculate Acitivity of a Source from Counting Rates in Single and Coincidence Photopeaks (Letter to the Editor). Accepted 5/9/77.
K. J. van Damme

Reply. Accepted 5/9/77.
Paul V. Harper and Katherine A. Lathrop

Oblique Views in Lung Perfusion Scanning: Clinical Utility and Limitations. Accepted 5/10/77.
Peter E. Nielsen, Peter T. Kirchner, and Frederick H. Gerber

Two Crystal Coincidence Counting of I-123 (Letter to the Editor). Accepted 5/11/77.
G. A. Brinkman and L. Lindner

Reply. Accepted 5/11/77.
Pantelis D. Mpanias, Daniel A. Gollnick, Wai-Nang P. Lee, and Moses A. Greenfield

Skeletal Uptake of Tc-99m HEDP in Primary Hyperparathyroidism (Letter to the Editor). Accepted 5/11/77.
I. Fogelman, W. R. Greig, R. G. Bessent, and I. T. Boyle

Myocardial Uptake of Tc-99m Skeletal Agents in the Rat After Experimental Induction of Microscopic Foci of Injury. Accepted 5/19/77.
D. G. Miller, R. F. Gilmour, Z. D. Grossman, S. Mallov, B. W. Wistow, and R. F. Rohner

Bone Scan Appearance of a Paget's Osteosarcoma: Failure to Concentrate HEDP (Letter to the Editor). Accepted 5/19/77.
J. H. McKillop, I. Fogelman, I. T. Boyle, and W. R. Greig

Iodinated *E. coli* 70S Ribosomes as a Radiocolloid of Uniform Particle Size for Lymph-Node and Liver Scanning (Concise Communication). Accepted 5/19/77.
A. S. K. Chan, A. Warbick, G. N. Ege, and F. P. Ottensmeyer

Parathyroid Adenoma Imaged by Ga-67 Citrate Scintigraphy (Case Report). Accepted 5/20/77.
C. Bekerman, J. A. Schulak, E. L. Kaplan, and K. Shen

A Comparative Evaluation of Techniques for Rapid and Efficient In Vivo Labeling of Red Cells with [^{99m}Tc] Pertechnetate. Accepted 5/25/77.
Robert G. Hamilton and Philip O. Alderson

A Case of Myocardial Abscess Evaluated by Radionuclide Techniques (Case Report). Accepted 5/25/77.
Stewart M. Spies, Sheridan N. Myers, Vincent Barresi, I. Martin Grais, and Arthur DeBoer

Indium-11-Tagged Cellular Blood Components: Mechanism of Labeling and Intracellular Location in Human Neutrophils. Accepted 5/25/77.
Mathew L. Thakur, Anthony W. Segal, Louis Louis, Michael J. Welch, John Hopkins, and Timothy J. Peters

Hepatic Uptake of Tc-99m-Labeled Diphosphonate in Amyloidosis (Case Report). Accepted 6/13/77.
J. A. Vanek, S. A. Cook, and R. M. Bukowski